Backward Raman Amplification in a Plasma Waveguide

C.-H. Pai,[1,2,3] M.-W. Lin,[1,3] L.-C. Ha,[1,2,3] S.-T. Huang,[1,3,4] Y.-C. Tsou,[1,3] H.-H. Chu,[3] J.-Y. Lin,[4] J. Wang,[1,2,3] and S.-Y. Chen[1,3]

[1]*Institute of Atomic and Molecular Sciences, Academia Sinica, Taipei 106, Taiwan*
[2]*Department of Physics, National Taiwan University, Taipei 106, Taiwan*
[3]*Department of Physics, National Central University, Jhongli 320, Taiwan*
[4]*Department of Physics, National Chung Cheng University, Chia-Yi 621, Taiwan*

(Received 21 November 2007; published 8 August 2008)

Backward Raman amplification of a short laser pulse in a plasma waveguide is demonstrated. With a guided seed pulse of 0.8-μJ energy and a pump pulse of 345-mJ energy in a 9-mm-long optically preformed plasma waveguide, 910-fold energy amplification is achieved. Heating of the plasma by the long pump pulse is identified to be a key issue for plasma-waveguide-based backward Raman amplifiers.

DOI: 10.1103/PhysRevLett.101.065005 PACS numbers: 52.38.Bv, 52.35.Mw, 52.50.Jm

The development of laser systems towards higher and higher peak power has pushed forward the frontier of physics research and brought many novel applications in the past two decades. However, material breakdown caused by the laser field in laser amplifiers and compressors puts a major limitation on the progress. To overcome this obstacle, a plasma-based amplification scheme was proposed, in which a short seed pulse is amplified by a counterpropagating long pump pulse of shorter wavelength via plasma electron grating driven by beating of the two laser pulses. The plasma-based amplification scheme can be operated in two different regimes. In the backward Raman amplification (BRA) regime [1], the beat pattern of the pump and seed pulses resonantly excites a plasma wave with a plasma frequency matching the frequency difference of the two laser pulses. The plasma wave backscatters and down-shifts the pump pulse to increase the energy of the seed pulse. In the superradiant amplification (SRA) regime [2], the ponderomotive force of the beat pattern is sufficiently strong to dominate over the electrostatic force resulting from charge separation to drive a transient plasma grating. Under such a condition frequency matching is not a prerequisite. The threshold for transition from BRA to SRA is given by $\omega_b > \omega_p$ [2], where $\omega_b = 2\sqrt{a_0 a_1 \omega_0 \omega_1}$ is the bouncing frequency, ω_p is the plasma frequency, a_0 and a_1 are the amplitude of normalized vector potentials of the pump and seed pulses, and ω_0 and ω_1 are the laser frequencies. Recent developments in theory proposed that an appropriate combination of detunings of plasma density gradient and pump chirp can suppress the premature backscattering of the pump pulse caused by noise [3], the near-forward Raman scattering of the amplified seed pulse [4], and the superluminous precursor of the amplified seed pulse [5], all of which set serious limitations on BRA and SRA. Furthermore, it was proposed to use a plasma waveguide for dramatically increasing the energy transfer between the pump and seed pulses through the increase of the effective interaction length [6].

Experimentally, Ping *et al.* first demonstrated BRA in the linear regime with eightfold energy amplification by using a pump of 150-mJ energy and 5-ns pulse duration in a microcapillary preionized by another laser pulse [7]. Later, BRA with 95-fold energy amplification was reported with a 500-fs broadband seed pulse of 8-μJ energy and a 10-ps pump pulse of 20-mJ energy in a 2-mm gas jet [8]. Recently, the nonlinear regime of BRA was demonstrated with a narrowband seed of 7.5-μJ energy and 550-fs duration and a pump of 40-mJ energy and 10-ps duration [9], showing the characteristic gain saturation and temporal compression. A double-pass design was later demonstrated to increase the effective amplification length [10]. The first experimental demonstration of SRA was reported by Dreher *et al.* with 19-fold amplification [11]. The SRA mechanism is verified by the observation of breakup of the amplified seed pulse into a sequence of pulses separated by $2\pi/\omega_b$. To date, no experimental demonstration of BRA or SRA in a plasma waveguide is reported. In this Letter, we report demonstration of backward Raman amplification in an optically preformed plasma waveguide. By using the ignitor-heater scheme [12,13] to produce a 9-mm-long plasma waveguide in a hydrogen gas jet, 910-fold energy amplification is achieved with a guided seed pulse of 0.8-μJ energy and a pump pulse of 345-mJ energy. The mechanism of BRA is identified through the locking of the central wavelength of the amplified seed pulse to the Raman satellite frequency and the shrink of the bandwidth with increasing interaction length. The advantages of using a plasma waveguide for BRA and the limitations of our current implementation are addressed.

A 10-TW, 38-fs, 810-nm, and 10-Hz Ti:sapphire laser system based on chirped-pulse amplification technique with a bandwidth of 30 nm (upgraded from the laser system in Ref. [14]) is used for this experiment. Two laser pulses, referred to as the ignitor and the heater, are used for producing a plasma waveguide. The 38-fs *p*-polarized ignitor has an energy of 75 mJ and the 160-ps *s*-polarized heater has an energy of 300 mJ. The ignitor-

heater separation is 200 ps. After combined by a thin-film polarizer, these two pulses propagate collinearly and are then focused by an axicon of 30° base angle to a line focus of >2-cm length in full width at half maximum (FWHM). A hole of 5-mm diameter at the center of the axicon and another at the center of the turning mirror before the axicon allow passage of the pump pulse. To increase the efficiency of waveguide fabrication a convex lens of 40-cm focal length with a hole of 2-cm diameter at the center is put before the axicon to concentrate the laser energy in ~1-cm length and to optimize the uniformity of longitudinal intensity distribution. The p-polarized pump pulse is an uncompressed pulse with 810-nm central wavelength, 160-ps duration, positive chirp, and a maximal energy of 345 mJ. It is focused with an $f/7$ off-axis parabolic mirror onto one end of the plasma waveguide (referred to as the pump entrance or the seed exit) with its propagation path collinear to the waveguide. The focal spot size is 10 μm FWHM with 85% energy enclosed in a Gaussian-fit profile. The p-polarized seed pulse is focused with an $f/10$ lens onto the other end of the plasma waveguide (referred to as the seed entrance or the pump exit) and propagates in the opposite direction of the pump pulse. The focal spot size is 14-μm FWHM with 80% energy enclosed in a Gaussian-fit profile. The seed pulse is generated from supercontinuum generation of a short 810-nm 320-μJ laser pulse in a krypton gas cell and then compressed by a 4-f phase compensator [15]. The central wavelength and bandwidth of the seed pulse are tunable by adjusting the position and width of a slit located close to the liquid-crystal spatial phase modulator in the 4-f phase compensator.

The hydrogen gas jets are produced by a pulsed valve with various slit nozzles. Two flat-topped gas jets are used in this experiment, one of 9-mm length and the other of 4-mm length, both with a width of 600 μm. The gas-jet atom density is fixed at 4.0×10^{19} cm^{-3} with a backing pressure of 6.0×10^{6} Pa. The energy and beam profile of the transmitted pump pulse is measured by a relayed imaging system with a charge-coupled-device (CCD) camera, after passing through a dichroic mirror. The transmitted seed pulse is recollimated by the pump parabolic mirror, picked out by a dichroic mirror, and then sent to another relayed imaging system of calibrated sensitivity for measuring the energy and beam profile at the interaction region or directed to a spectrometer. Mach-Zehnder interferometry with a 38-fs probe pulse passing transversely through the gas jet is used to measure the plasma density distribution.

The plasma waveguide is produced by using the axicon-ignitor-heater scheme [12], in which a short ignitor pulse provides seed electrons via multiphoton ionization and a subsequent long high-energy heater pulse heats up the plasma through inverse bremsstrahlung heating and further ionizes the gas through collisional ionization. The resultant line-shaped hot dense plasma expands, yielding a reduced on-axis plasma density, and the outgoing plasma ionizes the gas in the encircling outer region through collision. After an adequate delay (e.g., a few ns for the axicon heater pulse used in this experiment) the plasma electron density in the encircling outer region becomes larger than the on-axis density and thereby a plasma waveguide capable of guiding a laser pulse is produced.

Figure 1(a) shows the interferogram for using only the pump pulse of 345-mJ energy taken at 90 ps after the passage of the peak of the pump pulse through the 9-mm gas jet, (b) shows the interferogram for the waveguide produced by the ignitor and heater pulses taken at 2.1 ns

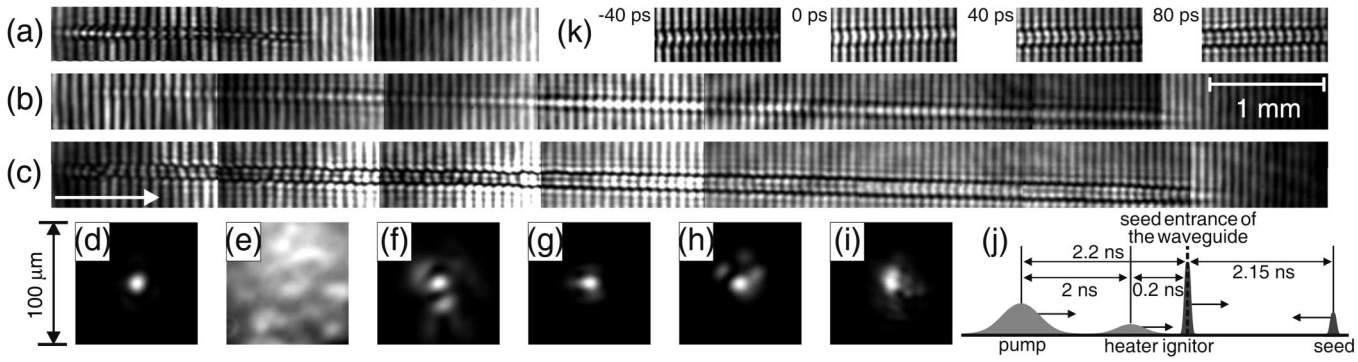

FIG. 1. Interferograms taken at 90 ps after the peak of the 345-mJ pump pulse has passed through the 9-mm gas jet, (a) with only the pump pulse, (b) with only the 75-mJ ignitor pulse and the 300-mJ heater pulse for an ignitor-heater separation of 200 ps, and (c) with the pump pulse guided by the plasma waveguide shown in (b). The gas atom density is 4.0×10^{19} cm^{-3} and the heater-pump delay is 2 ns. The insets shows the beam profiles of (d) the pump pulse at the pump entrance of the waveguide, (e) the pump pulse at the pump exit of the gas jet without the waveguide, (f) the pump pulse at the pump exit of the waveguide, (g) the seed pulse at the seed entrance of the waveguide, (h) the seed pulse at the seed exit of the waveguide without the pump pulse, and (i) the seed pulse at the seed exit of the waveguide with the pump pulse. (j) Relative timing of the four laser pulses at the seed entrance of the waveguide. (k) Interferograms for the middle of the plasma waveguide at various probe delays with respective to the peak of pump pulse. The central wavelength of the seed is 869 nm and the seed pulse arrives at the seed entrance of the waveguide at 50 ps before the arrival of the peak of the pump pulse at the same position. The white arrow indicates the direction of pump propagation.

after the heater pulse, and (c) shows the interferogram taken at 90 ps after the passage of the peak of the pump pulse through the waveguide shown in (b) with a heater-pump delay of 2 ns. Figure 1(d) shows the profile of the pump pulse at the pump entrance of the waveguide, (e) shows the pump-pulse profile at the pump exit of the gas jet without the waveguide, and (f) shows the profile with the plasma waveguide. Although for Fig. 1(b) the transverse density profile of the plasma waveguide cannot be correctly retrieved from the interferograms due to the limited resolution and the small channel diameter, guiding of the pump pulse in the waveguide can be verified from the shrink of the pump beam size at the pump exit of the waveguide to <30 μm. Figure 1(g) shows the seed-pulse profile at the seed entrance of the waveguide, (h) shows the profile at the seed exit of the waveguide without the pump pulse, and (i) shows the profile with the pump pulse. Figure 1(j) illustrates the relative timing of the four laser pulses at the seed entrance of the waveguide. The seed pulse arrives at the seed entrance of the waveguide at 50 ps before the arrival of the peak of the pump pulse at the same position. Guiding of the seed pulse in the waveguide is verified from the shrink of the seed beam size at the seed exit of the waveguide and also from its amplification by the pump pulse. The interferograms are roughly the same for the cases with and without the seed pulse.

It can be seen clearly from Figs. 1(b) and 1(c) that the guided pump pulse significantly changes the characteristics of the waveguide in the time scale of pump-pulse duration. A sequence of interferograms for the middle of the plasma waveguide taken at various probe delays [Fig. 1(k)] show that the waveguide evolves significantly during passage of the long pump pulse. The calculated plasma temperature resulting from inverse bremsstrahlung heating by the pump pulse is 150 eV when the seed is at the seed entrance of the waveguide and 210 eV when the seed is at the seed exit. The time scale for hydrodynamic evolution of the plasma waveguide is w_0/c_s [16], where w_0 is the waveguide diameter, $c_s = (\langle Z \rangle T_e/m_i)^{1/2}$ is the sound speed, and $\langle Z \rangle$, T_e, and m_i are the average ion charge, the electron temperature, and the ion mass, respectively. The time scale given by w_0/c_s is 70–85 ps during passage of the seed pulse. Consequently the pump pulse also serves as an additional heater pulse which leads to rapid evolution of the waveguide even within the time scale of seed amplification. As a result, the rear part of the pump pulse encounters a waveguide of lower on-axis density and larger channel diameter.

Figure 2(a) shows the spectra of the amplified seed for input seed of various spectra with different central wavelengths. The other parameters are the same as that in Fig. 1. It is found that for all the conditions with significant amplification the central wavelength of the amplified seed is locked to the range of 859–867 nm. This is consistent with the wavelength of Stokes Raman satellite

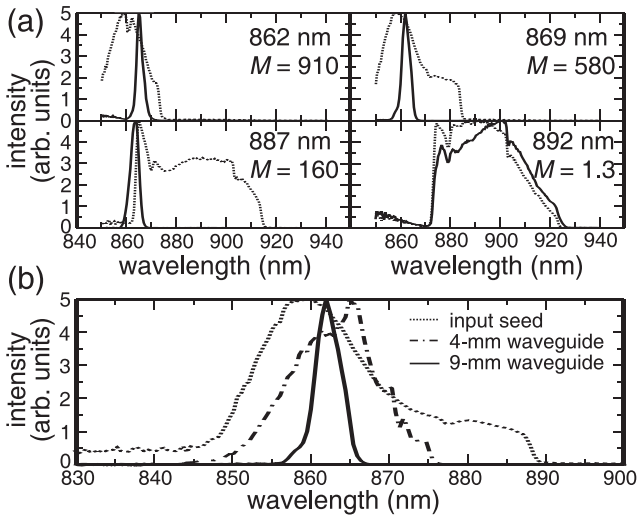

FIG. 2. (a) Spectra of the amplified seed pulse for input seed of various spectra with different central wavelengths. The other parameters are the same as that in Fig. 1. The number M is the amplification factor of each case. (b) Spectra of the input seed, the amplified seed with the 4-mm plasma waveguide, and the amplified seed with the 9-mm plasma waveguide. The central wavelength of the seed is 869 nm.

corresponding to the on-axis density of the plasma waveguide retrieved from the interferograms ($\sim 5.9 \times 10^{18}$ cm^{-3}, corresponding to the first-order Stokes wavelength at 861 nm) for the middle of the waveguide upon seed arrival. This reveals that backward Raman amplification is the dominant mechanism in this experiment. The small variation of the central wavelength of the amplified seed may be ascribed to shot-to-shot fluctuation of the on-axis density. Figure 2(a) also shows the energy amplification factor (the ratio between the energies of the seed pulse at the seed exit of the waveguide with and without the pump pulse) for each case. The largest energy amplification factor is 910, which occurs when the central wavelength of the seed pulse is 862 nm and the guided seed-pulse energy is 0.8 μJ. The amplification factor decreases with increasing central wavelength of the input seed, which can be simply ascribed to the reduction of effective seed energy in the bandwidth of resonance of the Stokes Raman satellite. If there is no energy in the input seed falling into the resonant band, such as in the lower right graph of Fig. 2(a), no amplification of seed is observed and the output seed spectrum is the same as that of the input seed. Note that the 30% amplification observed in this case is possibly due to the increased guiding efficiency resulting from the modification of the waveguide by the pump pulse.

Figure 2(b) shows the spectra of the input seed, the amplified seed with the 4-mm waveguide, and the amplified seed with the 9-mm waveguide. The central wavelength of the seed is 869 nm. The bandwidth of the amplified seed pulse decreases with increasing interaction

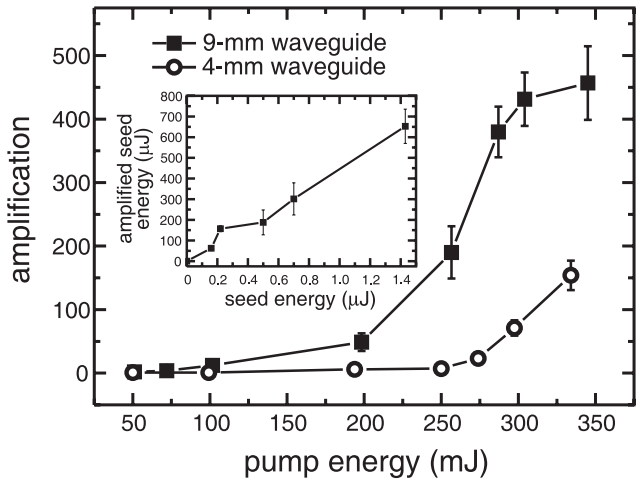

FIG. 3. Amplification factor as a function of pump energy for 1.4-μJ seed energy with the 9-mm gas jet and the 4-mm gas jet. The inset shows the amplified seed energy as a function of input seed energy for 345 mJ pump energy with the 9-mm gas jet. The central wavelength of the seed pulse is 869 nm. The other parameters are the same as that in Fig. 1. The data points represent averages of 5 laser shots and the error bars indicate the standard deviation.

length (from 12 nm for 4-mm waveguide to 4.4 nm for 9-mm waveguide), indicating that the backward Raman amplification is in the linear regime [1].

Figure 3 shows the amplification factor as a function of pump energy for 1.4-μJ seed energy and the inset shows the amplified seed energy as a function of input seed energy for 345-mJ pump energy. The central wavelength of the seed pulse is 869 nm. The other parameters are the same as that in Fig. 1. For the 4-mm gas jet the amplified seed energy shows an exponential dependence on pump energy and for the 9-mm gas jet it shows an exponential dependence of a larger slope with saturation at high pump energies. Because the seed pulse propagates in the direction opposite to the pump pulse, it encounters a waveguide of decreasing on-axis density and increasing channel diameter. Both the decrease of on-axis density and increase of channel diameter can lower the RBS growth rate and thus lead to the saturation. In addition, the detuning of the resonant Raman frequency with seed propagation due to the decreasing on-axis density becomes larger with increasing pump energy, which can also lead to a reduced growth rate. Furthermore, the increase of the plasma temperature due to heating by the pump pulse also leads to damping of the mediating plasma wave as a result of trapping and acceleration of the hot background electrons, the number of which increases with increasing temperature, and thus reduces the growth rate. Figure 3 shows that the ratio of the amplification factor with the 9-mm waveguide to that with the 4-mm waveguide is 27 for 250-mJ pump energy and becomes 3 for 345-mJ pump energy. This verifies that heating by the pump pulse does reduce the growth rate. Also, it is found that the amplification factor for the case with the seed entering the seed entrance of the waveguide at -50 ps and exiting at $+10$ ps with respect to the peak of the pump pulse is about 3 times larger than that for the case with the seed entering the seed entrance of the waveguide at -10 ps and exiting at $+50$ ps. This verifies that the adverse effect from the heating by the pump pulse is accumulative. The amplified seed energy shows a linear dependence on the input seed energy. This again indicates that the experiment is in the linear regime of BRA. The background signal produced by Raman backscattering instability of the pump pulse induced by noise is measured to be <5 nJ by turning off the seed.

In summary, backward Raman amplification in an optically preformed plasma waveguide is demonstrated, and energy amplification exceeding 900 fold is achieved by using a 9-mm waveguide. The limits on the pulse duration and energy of the amplified seed due to heating of the plasma waveguide by the pump pulse are the major issues of implementing a plasma waveguide for such an amplifier. Both limits may be mitigated if the SRA regime is reached, because for SRA frequency matching is not a prerequisite. On the other hand, the tapering of the on-axis density by the pump pulse may be exploited to suppress near-forward Raman scattering [4] and superluminous precursor [5] of the amplified seed pulse in a high-power amplifier.

[1] V. M. Malkin, G. Shvets, and N. J. Fisch, Phys. Rev. Lett. **82**, 4448 (1999).
[2] G. Shvets *et al.*, Phys. Rev. Lett. **81**, 4879 (1998).
[3] V. M. Malkin, G. Shvets, and N. J. Fisch, Phys. Rev. Lett. **84**, 1208 (2000).
[4] V. M. Malkin, Y. A. Tsidulko, and N. J. Fisch, Phys. Rev. Lett. **85**, 4068 (2000).
[5] Yu. A. Tsidulko, V. M. Malkin, and N. J. Fisch, Phys. Rev. Lett. **88**, 235004 (2002).
[6] P. Mardahl *et al.*, Phys. Lett. A **296**, 109 (2002).
[7] Y. Ping *et al.*, Phys. Rev. E **62**, R4532 (2000); Y. Ping *et al.*, *ibid.* **66**, 046401 (2002).
[8] Y. Ping *et al.*, Phys. Rev. Lett. **92**, 175007 (2004).
[9] W. Cheng *et al.*, Phys. Rev. Lett. **94**, 045003 (2005).
[10] J. Ren *et al.*, Nature Phys. **3**, 732 (2007).
[11] M. Dreher *et al.*, Phys. Rev. Lett. **93**, 095001 (2004).
[12] Y.-F. Xiao *et al.*, Phys. Plasmas **11**, L21 (2004).
[13] C. G. R. Geddes *et al.*, Nature (London) **431**, 538 (2004).
[14] H.-H. Chu *et al.*, Appl. Phys. B **79**, 193 (2004).
[15] A. M. Weiner *et al.*, Opt. Lett. **15**, 326 (1990).
[16] C. G. Durfee, III, J. Lynch, and H. M. Milchberg, Phys. Rev. E **51**, 2368 (1995).